Indirect study of the $^{12}C(\alpha,\gamma)^{16}O$ reaction via the $^{12}C(^7Li, t)^{16}O$ transfer reaction

N. Oulebsir,[1,2] F. Hammache,[1,*] P. Roussel,[1] M. G. Pellegriti,[1,†] L. Audouin,[1] D. Beaumel,[1] A. Bouda,[2] P. Descouvemont,[3] S. Fortier,[1] L. Gaudefroy,[4,‡] J. Kiener,[5] A. Lefebvre-Schuhl,[5] and V. Tatischeff[5]

[1]*Institut de Physique Nucléaire d'Orsay, UMR8608, IN2P3-CNRS, Université Paris sud 11, 91406 Orsay, France*

[2]*Laboratoire de Physique Théorique, Université Abderahmane Mira, 06000 Béjaia, Algeria*

[3]*Physique théorique et Mathématique, ULB CP229, B-1050 Brussels, Belgium*

[4]*Grand Accélérateur National d'Ions Lourds, BP55076, 14076 Caen Cedex 5, France*

[5]*CSNSM, IN2P3-CNRS, Université Paris sud 11, 91405 Orsay, France*

(Received 21 July 2011; revised manuscript received 26 February 2012; published 16 March 2012)

The $^{12}C(\alpha,\gamma)^{16}O$ reaction plays a crucial role in stellar evolution. The rate of this reaction determines directly the ^{12}C-to-^{16}O abundance ratio at the end of the helium burning phase of stars and consequently has a big effect on the subsequent nucleosynthesis and even on the evolution of massive stars. However, despite many experimental studies, the low-energy cross section of $^{12}C(\alpha,\gamma)^{16}O$ remains uncertain. The extrapolation of the measured cross sections to stellar energies ($E \sim 300$ keV) is made particularly difficult by the presence of the 2^+ ($E_x = 6.92$ MeV) and 1^- ($E_x = 7.12$ MeV) subthreshold states of ^{16}O. To further investigate the contribution of these two subthreshold resonances to the $^{12}C(\alpha,\gamma)^{16}O$ cross section, we determine their α-reduced widths via a measurement of the transfer reaction $^{12}C(^7Li, t)^{16}O$ at two incident energies, 28 and 34 MeV. The uncertainties on the determined α-spectroscopic factors and the α-reduced widths were reduced thanks to a detailed distorted-wave Born approximation analysis of the transfer angular distributions measured at the two incident energies. The R-matrix calculations of $^{12}C(\alpha,\gamma)^{16}O$ cross section using our obtained α-reduced widths for the 2^+ and 1^- subthreshold resonances lead to an $E1$ S factor at 300 keV of 100 ± 28 keV b, which is consistent with values obtained in most of the direct and indirect measurements as well as the NACRE collaboration compilation while the result for the $E2$ component S_{E2} (300 keV) $= 50 \pm 19$ keV b disagrees with the NACRE adopted value .

DOI: 10.1103/PhysRevC.85.035804 PACS number(s): 25.70.Hi, 25.40.Lw, 25.55.−e, 26.20.Fj

I. INTRODUCTION

The $^{12}C(\alpha,\gamma)^{16}O$ reaction plays a crucial role in stellar nucleosynthesis. In stars such as red giants, where the stellar core is in the helium-burning phase, the $^{12}C(\alpha,\gamma)^{16}O$ reaction follows the production of ^{12}C by the triple α process. The ratio of the yields of these two reactions determines directly the ^{12}C-to-^{16}O abundance ratio in stars at the end of their helium-burning phase. This ratio has important consequences for the nucleosynthesis of elements heavier than carbon [1,2], which are almost exclusively produced in this kind of stars. It has also, according to recent calculations of Tur *et al.* [3,4], significant effects on the core-collapse supernovae production yields for ^{26}Al, ^{44}Ti, ^{60}Fe and on the production factors of s-process nuclides between ^{58}Fe and ^{96}Zr. Finally, the ^{12}C-to-^{16}O abundance ratio has an influence on the subsequent stellar evolution of the massive stars [1,2]. It somehow determines the final fate of stars, black holes, neutron stars, or white dwarfs.

The rate of the triple α process is well determined (10%–15% uncertainty) while the $^{12}C(\alpha,\gamma)^{16}O$ reaction rate has an uncertainty of about ∼40% [5] despite the various experiments that studied it these last 4 decades. The $^{12}C(\alpha,\gamma)^{16}O$ reaction occurs at a temperature around 0.2 GK, which corresponds to the Gamow peak at 300 keV. At this energy, the cross section is expected to be of the order of $\sim 10^{-8}$ nb, which excludes any direct measurement. Though direct measurements [6] have been performed at energies down to 0.9 MeV (c.m.), the extrapolation to stellar energy remains difficult. Indeed, the α-capture cross section at 300 keV, which corresponds to the excitation energy region of ^{16}O around 7.46 MeV, is expected to be dominated by several contributions, the most important ones being the $E1$ and $E2$ transitions to the ground state through the low-energy tail of the broad resonant 9.6 MeV 1^- state and the high-energy tails of the two-subthreshold resonant states at 7.12 MeV 1^- and 6.92 MeV 2^+ of ^{16}O. Contributions from cascade transitions are expected to be small [7]. The two subthreshold states make the extrapolation complicated because their contributions to the $^{12}C(\alpha,\gamma)^{16}O$ cross section at 300 keV are not very well known because measurements of their α-reduced widths and so their α-spectroscopic-factors via α-transfer reactions, are spread over too-large a range of values [8]. Moreover, in the extrapolation, one has to take into account also the contribution of the nonresonant direct capture and all possible interference effects between the different resonances [9].

In view of the importance of $^{12}C(\alpha,\gamma)^{16}O$, we address in this paper the problem concerning the values of the α-reduced width of the two subthreshold states of ^{16}O at 6.92 and 7.12 MeV by performing a new determination of these quantities through an α-transfer reaction. The use of the α transfer to get spectroscopic factors has been debated as less secure than single-particle transfer. Hence, to reduce these doubts, we have first chosen the $(^7Li, t)$ transfer reaction

*Corresponding author: hammache@ipno.in2p3.fr

†Present address: Dipartimento di Fisica e Astronomia, Universitá di Catania and Laboratori Nazionali del Sud-INFN, Catania, Italy.

‡Present address: CEA, DAM, DIF, F-91297 Arpajon, France.

instead of the (^{6}Li, d) reaction because it has two advantages: (i) The multistep effects are less marked for the (^{7}Li, t) reaction than for (^{6}Li, d) one [10,11], and (ii) transfer cross sections to low-spin states should be enhanced because of the nonzero α angular momentum in ^{7}Li, allowing a better momentum matching. This was shown in the study of the transfer reactions ^{12}C(^{6}Li, d)^{16}O [12] and ^{12}C(^{7}Li, t)^{16}O [13]. Second, we have performed the ^{12}C(^{7}Li, t)^{16}O transfer-reaction measurements at two incident energies 28 and 34 MeV to select more thoroughly the distorted-wave Born approximation (DWBA) parameters and to check the stability of the results and the direct character of the present transfer reaction.

II. EXPERIMENTAL PROCEDURE AND RESULTS

The experiment was performed using a ^{7}Li^{3+} beam provided by the Orsay Tandem-Alto facility. The beam current was measured by using a Faraday cup connected to a calibrated charge integrator and the intensity was kept around 100 nA. A self-supporting enriched ^{12}C target with a thickness of 0.080 $\pm$ 0.004 mg/cm^2 and an initial purity of about 99.9% was used. During the experiment, the ^{12}C buildup was monitored (see below). Elemental target thickness was determined at the end of the experiment by an energy loss measurement from α particles emitted by an ^{241}Am source. The reaction products were analyzed with an Enge Split-pole magnetic spectrometer and detected at the focal plane by a 50-cm-long position-sensitive gas chamber and a ΔE proportional gas counter. Thanks to the ΔE versus position measurements, the identification of the tritons has been made unambiguously.

The tritons were detected at angles ranging from 0° to 31° in the laboratory frame corresponding to angles up to 44° in the center-of-mass frame. The energy resolution was about 40 to 75 keV depending on the scattering angle and the used angular aperture.

A calibrated telescope equipped with a ΔE-E silicon detectors placed at 35° in the scattering chamber was used for an overall control of the experiment and to monitor continuously the ^{12}C buildup. It was also used for the 0° measurement as a monitor of the beam intensity because the beam was stopped in a thick absorber placed inside the spectrometer.

Typical triton spectrum measured at $\theta_{\rm lab} = 11.5°$, between 6 and 11 MeV, is displayed in Fig. 1.

Peaks not explicitly labeled in Fig. 1 are assigned to impurities in the target. The selective population of the known α-cluster states, 2^+ (6.92 MeV) and 4^+ (10.35 MeV) indicates that the data are consistent with a direct α-transfer mechanism at forward angles. An indication of the nondirect transfer strength is the integrated differential cross section of the 2^- unnatural parity state at 8.87 MeV as this state cannot be formed by a direct α transfer. The cross section of this state is found to be about 3.8% of the 6.92-MeV 2^+ α-cluster state. This is close to that of the non-α-cluster 9.85-MeV 2^+ state, which was found to be 6% of the 6.92-MeV level. The population of the 9.58-MeV state was found to be a factor of about 1.6 smaller than that of 7.12-MeV state and they are both more populated than the transitions to the 8.87- and 9.85-MeV states. All these observations support the idea of a dominant direct mechanism.

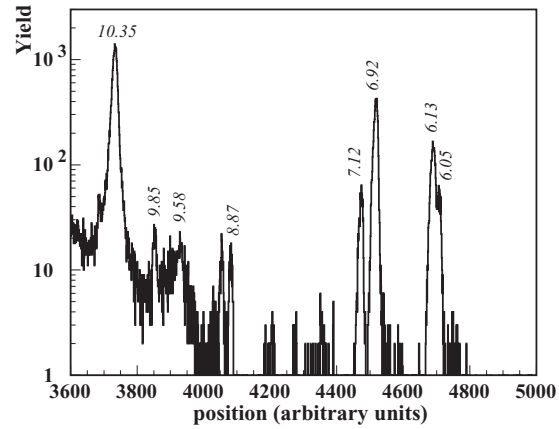

FIG. 1. Triton spectrum obtained at 11.5° (lab) with the 34-MeV ^{7}Li beam on ^{12}C target in the excitation energy region from 6 to 11 MeV. The excitation energy (MeV) of ^{16}O levels are indicated.

Data measured in the excitation energy region of the 2^- (8.87 MeV), 1^- (9.6 MeV), 2^+ (9.85 MeV), and 4^+ (10.35 MeV) states at 11.5° are displayed in Fig. 2 together with the three-level fit using a combination of Gaussian and Lorentzian functions used to extract the yields.

From the linewidth analysis of the 9.58- and 10.35-MeV peaks measured at different angles, we deduced a $\Gamma_{\rm c.m.}$ width of 349 $\pm$ 56 and 35 $\pm$ 8 keV, respectively. These values agree well with the results of the (^{7}Li, t) experiments of Becchetti *et al.* [13,14] and the recommended values of Tilley *et al.* [15].

From the measured triton yields, ^{12}C(^{7}Li, t)^{16}O differential cross sections corresponding to the 6.05-, 6.13-, 6.92-, 7.12-, 8.87-, 9.58-, 9.85-, and 10.35-MeV populated states of ^{16}O at the two incident energies of 28 and 34 MeV, were deduced. They are displayed in Fig. 3. The error bars assigned to our measured differential cross sections include the uncertainties on the peak yield, the number of target atoms, the solid angle and the integrated charge except for the zero degree run (no charge measurement) where the measured yield in the silicon monitor detector placed at 35° was used.

Note that measurements at 0° were only performed at the energy of 34 MeV because of the difficulties to perform easily

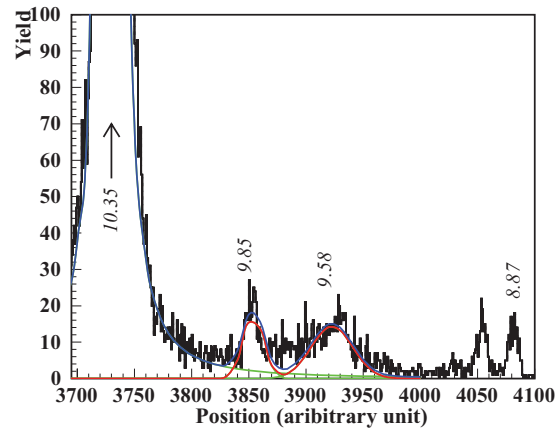

FIG. 2. (Color online) Three-level fit of the measured data for the 9.58-, 9.85-, and 10.35-MeV states in ^{16}O at $\theta_{\rm lab} = 11.5°$.

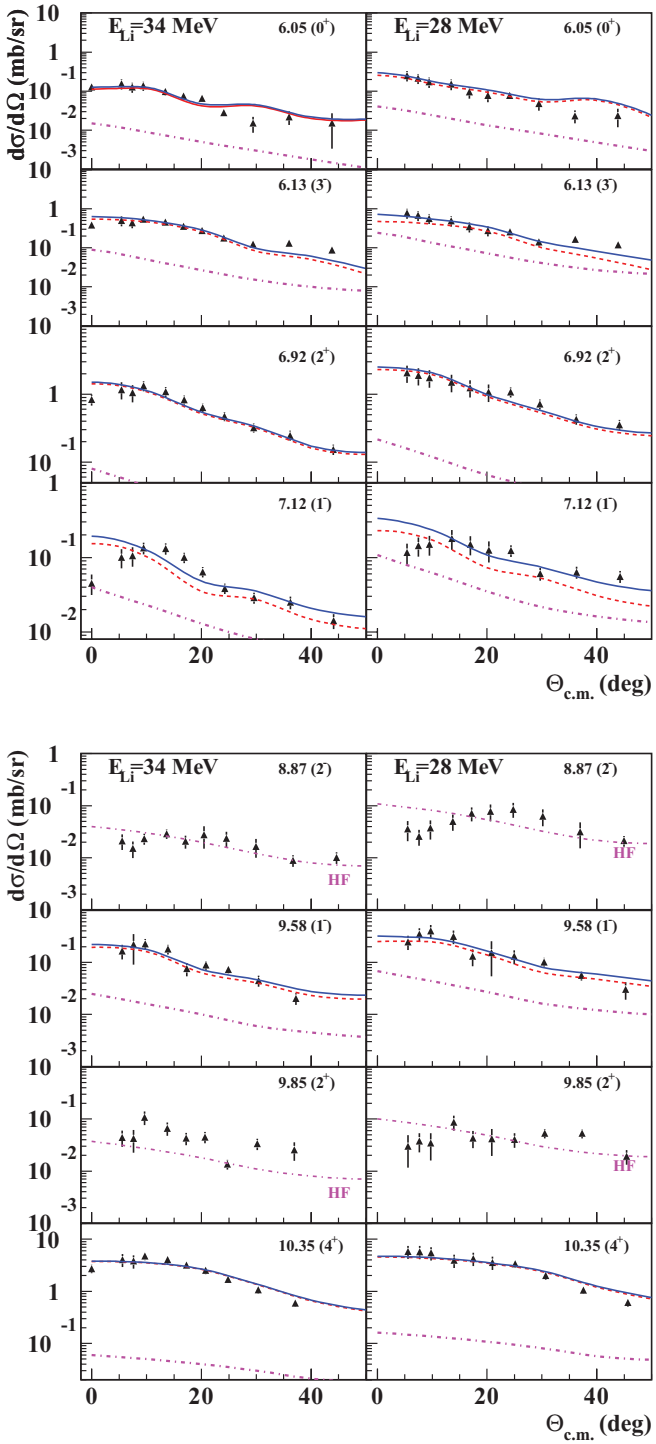

FIG. 3. (Color online) Experimental differential cross sections of the $^{12}C(^7Li,t)^{16}O$ reaction obtained at 34 MeV (left column) and 28 MeV (right column) for the 6.05-, 6.13-, 6.92-, 7.12-, 8.87-, 9.58-, 9.85-, and 10.35-MeV states, compared with FRDWBA calculations (dashed curve) normalized to the data, Hauser-Feshbach (HF) calculations (dashed-dotted line), and the sum HF + FRDWBA (solid line).

measurements at this angle. Moreover, no data points are displayed at 0° for the 8.87-, 9.58-, and the 9.85-MeV states at 34 MeV because the background was so important in this excitation energy range that the extraction of the yields for these states was meaningless.

III. DATA ANALYSIS AND DISCUSSIONS

The indication mentioned above of the relative dominant role of the direct mechanism in the $(^7Li,t)$ transitions supports the validity of a direct-reaction analysis of the angular distributions. However, the compound nuclear reaction contribution to all states has been also evaluated through Hauser-Feshbach calculations.

A. Hauser-Feshbach calculations

The observation of a non-natural parity 2^- state at 8.87 MeV indicates the presence of a non-negligible component of nondirect statistical compound nuclear (CN) reaction at both projectile energies because this level cannot be populated by a simple one-step direct α-transfer reaction. To determine the CN reaction contribution to all states, Hauser-Feshbach calculations were performed by considering $(^7Li,t)$ as triton evaporation from the compound nucleus ^{19}F. All the HF curves, displayed in Figs. 3 (left and right) as dashed-dotted lines, were normalized by a factor extracted from the ratio of the absolute values of the CN cross sections calculated for the 8.87-MeV state to those measured in this experiment. The cross section of all the states except the 8.87-MeV (2^-) and 9.85-MeV (2^+) levels exhibits a forward peaking shape at angles smaller than 20°, which is an indication of a direct mechanism. However, the comparison of Hauser-Feshbach calculation and the data for the 7.12-MeV state suggests that the latter has a non-negligible compound component, especially at the incident energy of 28 MeV, which will be taken into account in the analysis.

B. Finite-range distorted-wave Born approximation

Finite-range DWBA (FRDWBA) calculations, using the FRESCO code [16], were performed to extract the α-spectroscopic factor S_α from the data. Many combinations of entrance and exit optical potentials parameters were tested. Concerning the ^7Li channel, several ^7Li optical potentials were investigated within those given by Schumacher *et al.* [17]. For the triton exit channel, the selected optical potential parameters were taken from Garrett *et al.* [18]. The optical potential parameters finally selected are those giving the best fit for the whole studied transitions in the $(^7Li,t)$ reaction. These selected potentials are listed in Table I.

The dependence of our calculation on the $\alpha + ^{12}C$ Woods-Saxon (WS) interaction potential was investigated via the variation of the corresponding radius and diffuseness. A maximum likelihood function set at the 3σ level was used to select among the various interaction parameters used in our calculations, those giving the best fit of all the measured angular distributions of ^{16}O populated states (6.05, 6.13, 6.92, 7.12, 9.58, and 10.35 MeV) at both incident energies. This strong constraint led to a rather small range of the selected radius $r = 3.5$–4.5 fm and diffuseness $a = 0.53$–0.93 fm. The depth was adjusted to reproduce the binding energy of each considered ^{16}O bound state (41.7 and 40 MeV for 6.92- and 7.12-MeV states, respectively). Concerning the unbound

TABLE I. Optical Woods-Saxon potential parameters used for the FRDWBA analysis of $^{12}C(^{7}Li,t)^{16}O$ transfer reaction. The entrance-channel parameters 1A, 1B, and 1C are taken from Ref. [17]. The exit-channel parameters 2A and 2B are taken from Ref. [18].

Set	Channel	V (MeV)	r_r (fm)	a_r (fm)	W_V (MeV)	r_w (fm)	a_w (fm)
1A	$^{12}C+^{7}Li$	187.8	1.208	0.824	12.9	2.17	0.77
1B	—	245.0	1.210	0.759	14.7	2.00	0.909
1C	—	139.1	1.62	0.58	18.8	1.99	0.930
2A	$^{16}O+t$	162.9	1.16	0.69	17.9	1.5	0.82
2B	—	170.0	1.14	0.723	20.0	1.6	0.80

levels at the 9.58- and 10.35-MeV states, the calculations were performed at various positive α binding energies approaching zero and the resulting cross sections were then extrapolated to their real α-separation energy [13]. The number of radial nodes N were fixed by the oscillator energy conservation relation.

A comparison of FRDWBA calculations normalized to the extracted experimental data at the two incident energies are displayed in Figs. 3 (left and right) together with the Hauser-Feshbach calculations and the incoherent sum of HF and FRDWBA calculations. The displayed FRDWBA curves were obtained with the well parameters $r = 4.5$ fm and $a = 0.73$ fm and the optical potential parameters of the set 1C and 2B.

The good agreement between the calculations and the measured differential cross sections of the different excited states of ^{16}O at the two bombarding energies of 28 and 34 MeV, respectively, gives strong evidence of the direct nature of the $(^{7}Li,t)$ reaction populating most of the levels and confidence in our FRDWBA analysis. However, as one can see in Fig. 3, the agreement between the calculations and the data for the 7.12 MeV state is poor at angles smaller than 10° at both incident energies. This discrepancy is not understood and it was also observed in the $^{12}C(^{7}Li,t)^{16}O$ experiment of Becchetti *et al.* [13] at 34 MeV.

C. α-spectroscopic factors and comparison with previous transfer-reaction experiments

The α-spectroscopic factors were extracted from the normalization of the finite-range DWBA curves to the experimental data, $S_\alpha = \frac{\sigma_{exp}}{\sigma_{DW} S_\alpha^{^{7}Li}}$. The spectroscopic factor for the overlap between $\alpha + t$ and ^{7}Li was taken to be 1.0 [19]. The obtained S_α values for the 6.92- and 7.12-MeV states of interest are 0.15 ± 0.05 and 0.07 ± 0.03, respectively. They are displayed in Table II together with the results obtained for the other populated states, 6.05, 6.13, 9.58, and 10.35 MeV of ^{16}O, and those coming from previous transfer reaction measurements and SU(3) shell-model calculations.

The uncertainty on the extracted α-spectroscopic factors for all the populated states was evaluated from the dispersion of the various deduced S_α values at the two incident energies and corresponding to the various selected optical and interaction potentials as discussed previously. With the set of parameters (see above) selected by the χ^2 minimization on the whole range of measured angles and maximum likelihood tests, a maximum spreading of 15% on the S_α values was found when varying the entrance and exit optical potential parameters and considering both incident energies. A spreading of 33% for the 6.92-MeV state and 43% for the 7.12-MeV state was found when the well geometry parameters were varied. For any given set of selected parameters, we observe a decrease of S_α by 12% when the incident energy varies from 28 to 34 MeV, which is within the usual uncertainties of DWBA results.

Our deduced S_α mean values, for the states of interest at 6.92 and 7.12 MeV as well as the 6.05-, 6.13-, 9.58-, and 10.35-MeV states of ^{16}O are in very good agreement with that obtained in $^{12}C(^{7}Li,t)^{16}O$ experiment at 34 MeV of Becchetti *et al.* [13], as one can see in Table II. Our results for the 7.12-, 6.05-, and 10.35-MeV states are also in agreement with those coming from $^{12}C(^{6}Li,d)^{16}O$ experiment at 48 MeV of Belhout *et al.* [8] while the results for the 6.92-, 6.13-, and 9.58-MeV states were found, respectively, two, five, and three times smaller than Belhout *et al.* [8] ones. One can see also that our results are in disagreement with the results inferred from the $^{12}C(^{6}Li,d)^{16}O$ experiment at 42 MeV [20] and 90 MeV [14] of Becchetti *et al.* and from $^{12}C(^{7}Li,t)^{16}O$ at 38 MeV of Cobern *et al.* [21].

Concerning the Cobern *et al.* [21] results, one should point out that their obtained energy resolution was between 120 and 180 keV (use of silicon detectors), which implies a very poor separation, if not no separation, of the two states of interest, 6.92 and 7.12 MeV. This enhances the uncertainties on the determination of the populated yields of the two states, which

TABLE II. Comparison of the α-spectroscopic factors for the 6.92-, 7.12-, 6.05-, 6.13-, 9.58- and 10.35- MeV states of ^{16}O obtained in various experiments and this work.

Experiment	S_α 6.92 MeV, 2^+	S_α 7.12 MeV, 1^-	S_α 6.05 MeV, 0^+	S_α 6.13 MeV, 3^-	S_α 9.58 MeV, 1^-	S_α 10.35 MeV, 4^+	Reaction or theory	Energy (MeV)
This work	0.15 ± 0.05	0.07 ± 0.03	$0.13^{+0.07}_{-0.06}$	0.06 ± 0.04	$0.10^{+0.08}_{-0.06}$	$0.19^{+0.17}_{-0.08}$	$^{12}C+^{7}Li$	28, 34
Belhout [8]	0.37 ± 0.11	0.11 ± 0.03	0.12 ± 0.04	0.29 ± 0.15	0.34 ± 0.10	0.11 ± 0.06	$^{12}C+^{6}Li$	48
Becchetti [13]	$0.17^{+0.06}_{-0.04}$	$0.08^{+0.04}_{-0.06}$	$0.11^{+0.05}_{-0.02}$	$0.09^{+0.03}_{-0.06}$	$0.17^{+0.06}_{-0.03}$	$0.30^{+0.10}_{-0.06}$	$^{12}C+^{7}Li$	34
Becchetti [20]	1.35	$1.08^{+2.16}_{-0.68}$	0.81,0.945	1.08 (1.62-3.78)	$0.81^{+0.27}_{-0.40}$	0.4–0.54	$^{12}C+^{6}Li$	42
Becchetti [14]	4.134	2.6	3.58	3.66	2.37	3.9	$^{12}C+^{6}Li$	90
Cobern [21]	1.10	0.20	—	—	—	1.8	$^{12}C+^{7}Li$	38
Ichimura [22]	0.234	0.0468	0.244	0.0444	0.245	0.207	SU(3)	—
Strottman [23]	0.177	—	0.186	—	—	0.149	SU(3)	—

leads to an inaccurate determination of the differential transfer cross sections. Concerning the S_α of about 1.8 obtained for the 10.35-MeV state which is 16 and 6 times larger than our value and that of Becchetti [20], respectively, the authors [21] were suspicious about the result and they claimed that the evaluation of the transfer integral for the unbound states is very dependent on the extrapolation used for the final-state wave function and on the choice of cutoff radius.

As for $^{12}C(^6Li,d)^{16}O$ experiments at 42 and 90 MeV, Becchetti *et al.* [14,20] pointed out that their absolute S_α values for low l transfers are very model dependent and vary by a factor of about 10 or more when using various parameter sets. These huge variations are likely attributable to the poor momentum matching in the $(^6Li,d)$ reaction at 42 and 90 MeV, $\Delta L \approx 6\hbar$ and $\Delta L \approx 10\hbar$, respectively, and unlike $(^7Li,t)$, the $l = 0$ α angular momentum in ^{6}Li does not allow a better momentum matching. Moreover, the entrance optical potential parameters used in Refs. [14,20] were those extracted from the analysis of the elastic data at 50.6 and 99 MeV, respectively, different from the incident energies for the transfer reaction.

In our $^{12}C(^7Li,t)^{16}O$ experiment at 34 and 28 MeV, the momentum matching is much better, $\Delta L \approx 0$–$3\hbar$ on one hand, and on the other hand the entrance optical potential parameters used were constrained by the elastic measurements at 34 MeV of Schumacher *et al.* [17]. This enhances the confidence in our DWBA analysis of the data and thus on the obtained results.

A comparison of our results with those predicted by the SU(3) shell-model calculations of Refs. [22,23] is also given in Table II. SU(3) results of Ref. [23] are in very good agreement with our results, while those of Ref. [22] agree very well only for the 7.12-, 6.13-, and 10.35-MeV states of ^{16}O.

D. ANCs and α-reduced widths

The asymptotic normalization factors (ANCs) were deduced by using the following expression [24]:

$$\tilde{C}^2 = S_\alpha \frac{R^2\varphi^2(R)}{\tilde{W}^2(R)}, \tag{1}$$

where R is the α-^{12}C channel radius, φ is the radial part of the α-^{12}C cluster wave function, and $\tilde{W}(R)$ is the Whittaker function.

The obtained values for $R = 6.5$ fm where the wave function reaches its asymptotic value whatever the potential used among the selected optical and interaction potentials (see Sec. III B) are $\tilde{C}^2 = (2.07 \pm 0.80)10^{10}$ fm^{-1} and $\tilde{C}^2 = (4.00 \pm 1.38)10^{28}$ fm^{-1} for the 6.92- and 7.12-MeV states, respectively. They are found in good agreement with those obtained by Brune *et al.* [25], who deduced the ANCs and the α widths of the states of interest via a sub-Coulomb $^{12}C(^7Li,t)^{16}O$ and $^{12}C(^6Li,d)^{16}O$ ANC measurements (see Table III).

Concerning our evaluated uncertainties of about 38% for the 6.92-MeV state and 35% for the 7.12-MeV state on $\tilde{C}^2$, the values are different than those given for S_α because the variation of the well parameters leads to a change on S_α and $\varphi(R)$, which both contribute to a variation on $\tilde{C}^2$ (see the formula above). One has to notice that the same parameters must be used to derive the spectroscopic factor, the asymptotic wave function, and the ANC. The above statements are also true for the α-reduced widths of about 26.7 ± 10.3 keV and 7.8 ± 2.7 keV for the 6.92- and 7.12-MeV states, respectively, deduced by using the following expression [13]:

$$\gamma_\alpha^2 = \frac{\hbar^2 R}{2\mu} S_\alpha |\varphi(R)|^2, \tag{2}$$

where μ is the reduced mass and $\varphi(R)$ is the radial part of the α-^{12}C cluster wave function calculated at the channel radius $R = 6.5$ fm.

Concerning the other populated states, the deduced α-reduced widths are 19.7 ± 5.5, 2.35 ± 0.8, 30.4 ± 21.7, and 20.1 ± 7.9 keV for the 6.05-, 6.13-, 9.58-, and 10.35-MeV states, respectively. However, the values for γ_α^2 (9.58 MeV) and γ_α^2 (10.35 MeV) are less reliable as based on DWBA calculations for unbound states. So the adopted values for these two states are those deduced from the $\Gamma_{c.m.}$ ($\Gamma_\alpha = \Gamma_{c.m.}$) extracted from the linewidth analysis described above, namely γ_α^2 (9.6 MeV) $= 174 \pm 28$ keV and γ_α^2 (10.35 MeV) $= 60 \pm 14$ keV.

TABLE III. Comparison of the ANCs and the α-reduced widths for the 6.92 MeV (2^+) and 7.12 MeV (1^-) subthreshold states of ^{16}O obtained in this work and in [8,25] at 6.5 fm.

Experiment	$\tilde{C}^2(2^+)$ (10^{10} fm^{-1})	$\gamma_\alpha^2(2^+)$ (keV)	$\tilde{C}^2(1^-)$ (10^{28} fm^{-1})	γ_α^2 (1^-) (keV)
This work	2.07 ± 0.80	26.7 ± 10.3	4.00 ± 1.38	7.8 ± 2.7
Brune [25]	1.29 ± 0.23	—	4.33 ± 0.84	—
Belhout[a] [8]	—	98.8 ± 29.6	—	23.2 ± 8.8
Belhout[b] [8]	$1.96^{+1.41}_{-1.27}$	$26.6^{+19.2}_{-17.2}$	3.48 ± 2.00	4.59 ± 2.91

[a]Strict DWBA values.
[b]Normalized values.

IV. *R*-MATRIX CALCULATIONS AND RESULTS

The present values of γ_α^2 have been included in R-matrix calculations using the Descouvemont R-matrix code. Both $^{12}C(\alpha,\gamma)^{16}O$ S factors obtained by direct measurements at high energies and the phase shifts data from elastic scattering $^{12}C(\alpha,\alpha)$ measurements [26,27] were fitted. The $E1$ and $E2$ contributions were fitted separately and the best fits were determined through a χ^2 minimization. The input parameters in the fits are the "observed" values γ_α^2, Γ_α, and E_r (see Tables IV and V), which are converted to R-matrix parameters by using techniques of Angulo *et al.* [9].

For the $E2$ radiative capture process, the fits (see Figs. 4 and 5) were performed using four states including a background equivalent state. The four 2^+ levels consist in the subthreshold state at $E_x = 6.92$ MeV, the state at $E_x = 9.85$ MeV, the state at $E_x = 11.52$ MeV and a higher background equivalent state which represents the tails of other higher-lying 2^+ states. All the resonance parameters, except those describing the 2^+ background state are kept fixed (see Table IV) in the R-matrix calculation. For the

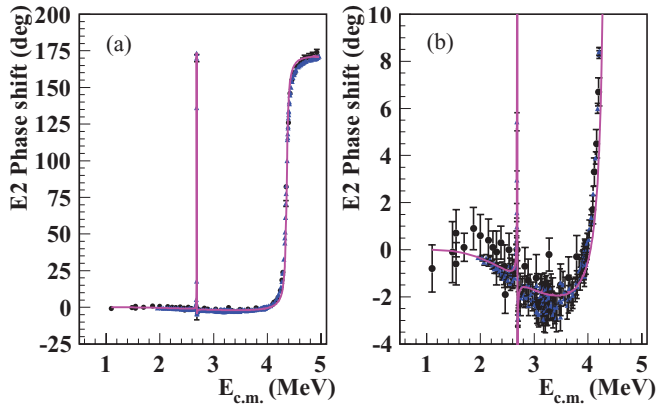

FIG. 4. (Color online) (a) Phase shifts for ^{12}C(α, α)^{12}C elastic diffusion reaction with R-matrix calculations of the $E2$ component. (b) Enlargement of the left figure. Data points are from Refs. [27] (black points) and [26] (blue triangles). The solid line corresponds to our best R-matrix fit with $\chi^2 = 1.02$.

α-reduced width of the 6.92 state, we fixed it to the value obtained in the present ^{12}C(^{7}Li, t)^{16}O measurement ($\gamma_\alpha^2 = 26.7 \pm 10.3$ keV) and its energy and Γ_γ were fixed to the values $E_r = -0.244\,85$ MeV and $\Gamma_\gamma = 97$ meV [15]. For the resonance properties of the $E_x = 9.85$ MeV and $E_x = 11.52$ MeV states, we used the values given in Ref. [26]. The fitting procedure was performed in two steps: First the excitation energy and the α-decay width of the 2^+ background state was determined from the best χ^2 fit of the phase shifts from Refs. [26,27] and then its γ-decay width was determined from the best χ^2 fit of the astrophysical S-factors data from Refs. [6,28–32].

The same procedure was performed for the $E1$ component with the fit of the phase shifts from Refs. [26,27] (see Fig. 6) followed by that of the astrophysical S-factors data from Refs. [6,28–33] (see Fig. 7) using this time

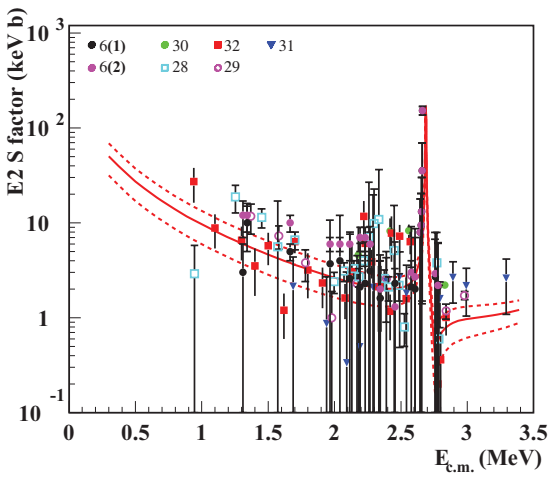

FIG. 5. (Color online) Astrophysical S factor for the ^{12}C(α,γ)^{16}O reaction with R-matrix calculations of the $E2$ component. Experimental data are from Refs. [6,28–32]. The solid line is our best R-matrix fit using our deduced γ_α^2 for the 6.92-MeV state and the dashed lines when using our upper and lower values for γ_α^2.

TABLE IV. Resonance parameters used in the R-matrix fit of the phase shifts and astrophysical S factors of the $E2$ component. The values in the brackets are the fixed resonance parameters.

J^π	E_x (MeV)	E_r (MeV)	γ_α^2 or Γ_α (keV)	Γ_γ (keV)
2^+	6.92	[−0.244]	$\gamma_\alpha^2 = [26.7 \pm 10.3]$	$[9.7 \times 10^{-5}]$
2^+	9.85	[2.683]	$\Gamma_\alpha = [0.76]$	$[5.7 \times 10^{-6}]$
2^+	11.52	[4.339]	$\Gamma_\alpha = [83.0]$	$[6.1 \times 10^{-4}]$
2^+	Background	7.0	$\gamma_\alpha^2 = 990$	2.2×10^{-4}

three levels. The three 1^- states consist of the subthreshold state at $E_x = 7.12$ MeV with fixed resonance parameters ($E_r = -0.0451$ MeV, $\Gamma_\gamma = 55$ meV [15], and our deduced $\gamma_\alpha^2 = 7.8 \pm 2.7$ keV), the state at $E_x = 9.585$ MeV with fixed parameters [15], and a higher background equivalent state which represents the tails of other higher-lying 1^- states with free parameters (see Table V).

An $E2$ S factor S_{E2} (0.3 MeV) of about 50 ± 19 keV b was obtained with the best fits shown in Fig. 4 ($\chi^2 = 1.02$) and Fig. 5 ($\chi^2 = 3.6$) and an $E1$ S factor S_{E1} (0.3 MeV) of about 100 ± 28 keV b was obtained with the best fits shown in Fig. 6 ($\chi^2 = 5.4$) and Fig. 7 ($\chi^2 = 2.35$).

To validate furthermore our R-matrix fits and results, especially for the $E1$ component, we performed a p-wave calculation of the β-delayed α-spectrum of ^{16}N. For the calculation, we used Eq. (3) of Ref. [34] and our R-matrix parameters of Table V while we considered the β-feeding amplitudes, A_{λ_l} (see Eq. (3) of Ref. [34]), as free parameters. Our calculation describes well, as one can see in Fig. 8, the measured data of Tang *et al.* [34] and this gives strong confidence in our R-matrix calculations. The disagreement between the calculation and the data in the energy region between 1.3 and 1.5 MeV is attributable to the f-wave contribution, which was not considered in the calculation because it is not contributing to the $E1$ component we are interested in.

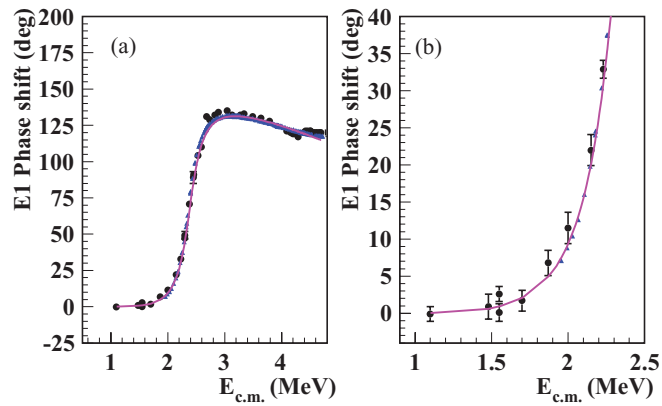

FIG. 6. (Color online) (a) Phase shifts for ^{12}C(α, α)^{12}C elastic diffusion reaction with R-matrix calculations of the $E1$ component. (b) Enlargement of the left figure. Data points are from [27] (black circles) and [26] (blue triangles). The solid line corresponds to our best R-matrix fit with $\chi^2 = 5.4$.

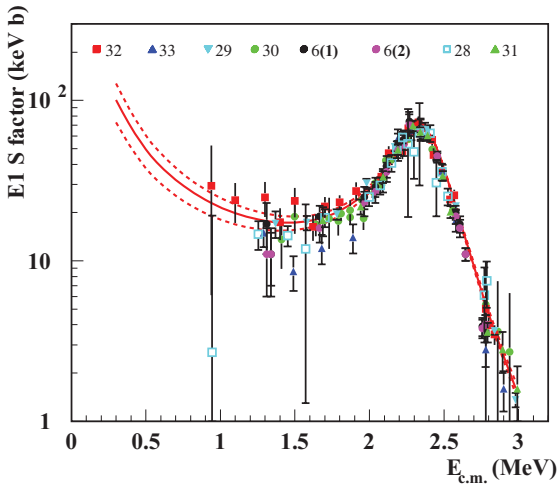

FIG. 7. (Color online) Astrophysical S factor for the $^{12}C(\alpha,\gamma)^{16}O$ reaction with R-matrix calculations of the $E1$ component. Experimental data are from Refs. [6,28–33]. The solid line is our best R-matrix fit using our deduced γ_α^2 for the 7.12-MeV state and the dashed lines when using our upper and lower values for γ_α^2.

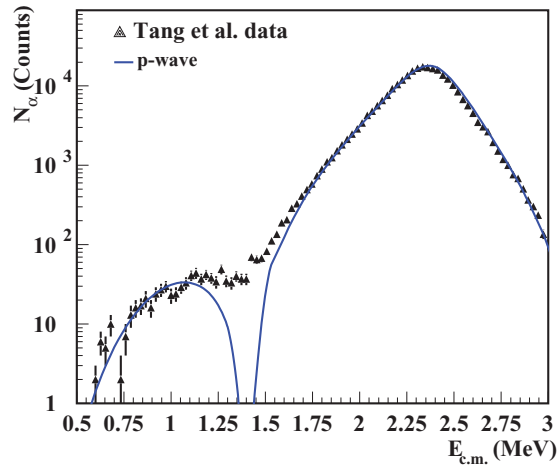

FIG. 8. (Color online) R-matrix calculation (see text) of the β-delayed α spectrum of ^{16}N together with data obtained in Ref. [34]. Only the p wave was considered in the calculation.

V. COMPARISON WITH PREVIOUS RESULTS

A comparison of the $E1$, $E2$, and total astrophysical S factors at 300 keV obtained in this work with the results obtained in previous works is given in Table VI.

Our value for the $E1$ component is in good agreement with the results obtained in various direct and indirect measurements [8,25,28,29,31,34–36] and with the value recommended in the NACRE compilation [5] (see Table VI) while our $E2$ component is in good agreement within the error bars with the values obtained in Refs. [25,26,28,29,36] but not with the value recommended in Ref. [5]. As one can see in Table VI, an excellent agreement of our central values with those obtained by Brune *et al.* [25] is observed for $E2$ and $E1$ components. We should note that in both works, the values of the α-reduced widths γ_α^2 or ANCs of the 6.92- and 7.12-MeV states were fixed in the R-matrix fitting procedure, which constrains more the calculations, while in other works they were considered as free parameters.

If we take for the cascade S factor the value 25^{+16}_{-15} keV b from Ref. [7], we obtain a total S factor, S (300 keV) $= 175 \pm 63$ keV b.

From the various compatible values for the $E1$ S factor at 300 keV tabulated in Table VI, a mean value of about S_{E1} (300 keV) $= 83 \pm 6$ keV b was deduced. For the $E2$ component, when considering only the $E2$ S factors that are in agreement, a mean value of about S_{E2} (300 keV) $= 43 \pm 5$ keV b was deduced. This led to a mean value for the total S factor of about 151^{+27}_{-26} when using the Matei *et al.* value [7] for the cascade S factor.

TABLE V. Resonance parameters used in the R-matrix fit of the phase shifts and astrophysical S factors of the $E1$ component. The values in the brackets are the fixed resonance parameters.

J^π	E_x (MeV)	E_r (MeV)	γ_α^2 or Γ_α (keV)	Γ_γ (keV)
1^-	7.12	[−0.0451]	$\gamma_\alpha^2 = [7.8 \pm 2.7]$	$[5.5 \times 10^{-5}]$
1^-	9.58	[2.416]	$\Gamma_\alpha = [388.0]$	$[1.56 \times 10^{-5}]$
1^-	Background	14.0	$\gamma_\alpha^2 = 2180.0$	5.0×10^{-4}

VI. CONCLUSION

In summary, the reaction $^{12}C(\alpha,\gamma)^{16}O$ was investigated through the direct α transfer reaction $(^7Li,t)$ at 28- and 34-MeV incident energies. The spectroscopic factors (and hence the α-reduced widths and the ANCs) of the ^{16}O subthreshold states at 6.92 (2^+) and 7.12 (1^-) MeV were deduced from a FRDWBA analysis using different sets of selected optical parameters. The uncertainties on the determined S_α and the deduced α-reduced widths and ANCs were reduced thanks to the constraints provided by the shape of our measured angular distributions of the various populated states of ^{16}O at the two incident energies. The obtained α-reduced widths

TABLE VI. Comparison of the astrophysical S factor at 300 keV obtained in various experiments, including this work, for the $E1$ and $E2$ components, as well as the total.

Experiment	S_{E1} (0.3 MeV) (keV b)	S_{E2} (0.3 MeV) (keV b)	S_{total} (0.3 MeV) (keV b)
This work	100 ± 28	50 ± 19	175^{+63}_{-62}
Brune [25]	101 ± 17	44^{+19}_{-23}	170^{+52}_{-55}
Belhout [8]	80^{+17}_{-16}	—	—
Tischauser [26]	—	53 ± 13	—
Tang [34]	84 ± 21	—	—
Azuma [35]	79 ± 21	—	—
Hammer [36]	77 ± 17	81 ± 22	183^{+55}_{-54}
Kunz [28]	76 ± 20	85 ± 30	186^{+66}_{-65}
NACRE [5]	79 ± 21	120 ± 60	224^{+97}_{-96}
Ouellet [29]	79 ± 16	36 ± 6	140^{+38}_{-37}
Rotters [31]	95 ± 44	—	—
Mean value	83 ± 6	43 ± 5	151^{+27}_{-26}

for the 2^+ and 1^-subthreshold resonances were introduced in the R-matrix fitting of radiative capture and elastic-scattering data to determine the low-energy extrapolations of $E2$ and $E1$ S factors. The result for the $E1$ S factor at 300 keV confirms the values obtained in various direct and indirect measurements as well as the NACRE compilation, while for the $E2$ component, the central value of our result is found to be nearly two times smaller than the NACRE recommended value. Our results are in excellent agreement with those of Brune *et al.* [25], and in both works the R-matrix fits were constrained by using fixed values for the α-reduced widths or the ANCs of the two subthreshold states.

ACKNOWLEDGMENTS

We would like to thank Nicolas de Séréville for his useful comments on the manuscript. We also wish to thank the Tandem-Alto staff and M. Vilmay for their strong support during the experiment.

[1] T. A. Weaver and S. E. Woosley, Phys. Rep. **227**, 65 (1993).
[2] M. Hashimoto, Prog. Theor. Phys. **94**, 663 (1996).
[3] C. Tur, A. Heger, and S. Austin, Astrophys. J. **718**, 357 (2010).
[4] C. Tur, A. Heger, and S. Austin, Astrophys. J. **702**, 1068 (2009).
[5] C. Angulo *et al.*, Nucl. Phys. A **656**, 3 (1999).
[6] M. Assunção *et al.*, Phys. Rev. C **73**, 055801 (2006), and references therein.
[7] C. Matei *et al.*, Phys. Rev. Lett. **97**, 242503 (2006).
[8] A. Belhout *et al.*, Nucl. Phys. A **793**, 178 (2007), and references therein.
[9] C. Angulo and P. Descouvemont, Phys. Rev. C **61**, 064611 (2000).
[10] K. W. Kemper and T. R. Ophel, Aust. J. Phys. **33**, 197 (1980).
[11] A. Bonaccorso and G. F. Bertsch, Phys. Rev. C **63**, 044604 (2001).
[12] P. T. Debevec *et al.*, Phys. Rev. C **9**, 2451 (1974).
[13] F. D. Becchetti and J. Jänecke, Nucl. Phys. A **305**, 293 (1978).
[14] F. D. Becchetti, D. Overway, and J. Jänecke, Nucl. Phys. A **344**, 336 (1980).
[15] D. R. Tilley, H. R. Weller, and C. M. Cheves, Nucl. Phys. A **564**, 1 (1993).
[16] I. J. Thomson *et al.*, Comput. Phys. Rep. **7**, 167 (1988).
[17] P. Schumacher *et al.*, Nucl. Phys. A **212**, 573 (1973).
[18] J. D. Garrett *et al.*, Nucl. Phys. A **212**, 600 (1973).
[19] M. G. Pellegriti, F. Hammache, P. Roussel *et al.*, Phys. Rev. C **77**, 042801 (2008), and references therein.
[20] F. D. Becchetti and J. Jänecke, Nucl. Phys. A **305**, 313 (1978).
[21] M. E. Cobern, D. J. Pisano, and P. D. Parker, Phys. Rev. C **14**, 491 (1976).
[22] M. Ichimura, A. Arima, E. C. Halbert, and T. Terasawa, Nucl. Phys. A **207**, 225 (1973); K. T. Hecht (private communication).
[23] D. Strottman and D. J. Millener, in *Proceedings of the International Conference on Nuclear Physics*, edited by J. de Boer and H. J. Mang (North-Holland, Amsterdam, 1973), Vol. 1, p. 107.
[24] A. M. Mukhamedzhanov and R. E. Tribble, Phys. Rev. C **59**, 3418 (1999).
[25] C. R. Brune, W. H. Geist, R. W. Kavanagh, and K. D. Veal, Phys. Rev. Lett. **83**, 4025 (1999), and references therein.
[26] P. Tischhauser *et al.*, Phys. Rev. C **79**, 055803 (2009).
[27] R. Plaga *et al.*, Nucl. Phys. A **465**, 291 (1987).
[28] R. Kunz, M. Jaeger, A. Mayer, J. W. Hammer, G. Staudt, S. Harissopulos, and T. Paradellis, Phys. Rev. Lett. **86**, 3244 (2001).
[29] J. M. Ouellet *et al.*, Phys. Rev. C **54**, 1982 (1996).
[30] P. Dyer *et al.*, Nucl. Phys. A **233**, 495 (1974).
[31] G. Rotters *et al.*, Eur. Phys. J. A **6**, 451 (1999).
[32] A. Redder *et al.*, Nucl. Phys. A **462**, 385 (1987).
[33] R. M. Kremer, C. A. Barnes, K. H. Chang, H. C. Evans, B. W. Filippone, K. H. Hahn, and L. W. Mitchell, Phys. Rev. Lett. **60**, 1475 (1988).
[34] X. D. Tang *et al.*, Phys. Rev. C **81**, 045809 (2010).
[35] R. E. Azuma *et al.*, Phys. Rev. C **50**, 1194 (1994).
[36] J. W. Hammer *et al.*, Nucl. Phys. A **752**, 514c (2005).